

## Zonally symmetric and asymmetric features of the tropospheric Madden-Julian oscillation

Mary T. Kayano

Instituto Nacional de Pesquisas Espaciais, São José dos Campos, São Paulo, Brazil

Vernon E. Kousky

Climate Prediction Center, National Centers for Environmental Prediction, Camp Springs, Maryland

**Abstract.** The evolving intraseasonal (IS) modes of the zonally symmetric (ZS) part (the latitudinal profile) of the 200-hPa stream function have been determined by performing extended empirical orthogonal function (EEOF) analyses for the northern hemisphere (NH) summer and winter. In each analysis the first EEOF mode describes an oscillation with a period of about 50 days. The prominent feature of the upper tropospheric stream function latitudinal profiles, for both seasons, is the propagation of the largest loadings in both hemispheres from near the equator toward higher latitudes. This propagation is more evident during the NH winter and throughout the year in the southern hemisphere (SH). In the NH the poleward propagation of the loadings is more conspicuous within the equator and the 30°N latitudinal band. The associated patterns for the zonally asymmetric (ZA) part of the sea level pressure and the 850- and 200-hPa zonal winds have also been determined. These patterns feature, in general, the largest correlations in the tropics and a large-scale zonal wavenumber one structure propagating continuously eastward around the globe with a 50-day period. The ZA patterns for certain variables show strong seasonal dependence. The 850-hPa ZA zonal wind patterns feature the largest correlations approximately along the climatological position of the Intertropical Convergence Zone, whereas the largest correlations for the upper level ZA zonal wind patterns are found near the equator, mainly in the winter hemisphere.

### 1. Introduction

Madden and Julian [1971, 1972], using spectral analysis of radiosonde observations, were the first to note a quasi-periodic 40- to 50-day intraseasonal (IS) oscillation in the tropical zonal wind and surface pressure. Subsequently, several authors presented observational evidence of the existence of this oscillation in the tropical atmosphere. The Madden-Julian oscillation (MJO) propagates eastward and is characterized by a zonal wavenumber one structure. The strongest signal in the convection occurs over the warmest water in the Indian and western Pacific Oceans [e.g., Lorenc, 1984]. The global aspects of the MJO, as evident in the outgoing longwave radiation (OLR) and the 250-hPa stream function and velocity potential, have been well documented [e.g., Weickmann, 1983; Weickmann *et al.*, 1985; Knutson *et al.*, 1986; Knutson and Weickmann, 1987; Kiladis and Weickmann, 1992]. In the equatorial latitudes the OLR and the 250-hPa velocity potential anomalies propagate continuously eastward, with the negative OLR anomalies being accompanied by upper level anomalous divergence. The eastward shift of the tropical convection is accompanied by variations in the subtropical atmospheric circulation, mainly in the regions of the Pacific and the Americas [e.g., Weickmann, 1983; Lau and Chan, 1985; Weickmann *et al.*, 1985; Madden, 1986; Knutson and Weickmann, 1987; Ghil and Mo, 1991a; Kiladis and Weickmann, 1992; Mo and Kousky, 1993; Madden and

Julian, 1994; Higgins and Mo, 1997]. Ghil and Mo [1991a, b] observed oscillations with similar periods in the zonal wind and geopotential height in the extratropics. They reported 40- to 50-day oscillations in several variables and latitudes and found that the midlatitude 40-day oscillation could be separate from the tropical MJO.

Another aspect of the MJO is its zonal-mean structure revealed in several variables. Using a zonally symmetric model, Anderson and Stevens [1987] suggested that the MJO might result from a combination of the zonally symmetric modes and the asymmetric traveling modes. The zonal-mean structure of the MJO relates to variations in the Earth's angular momentum, which result in variations in the length of day [e.g., Langley *et al.*, 1981; Anderson and Rosen, 1983]. Corresponding fluctuations in the atmospheric angular momentum (AAM) have also been observed [e.g., Langley *et al.*, 1981; Rosen and Salstein, 1983; Madden, 1987; Magaña, 1993]. Benedict and Haney [1988] and Gutzler and Madden [1993] showed that almost all the contribution to the 50-day oscillation in the AAM comes from variations in the zonal wind in the area equatorward of 20°. Kang and Lau [1990] suggested that the surface wind stress associated with the strengthening of the easterlies over central Pacific would be the major mechanism increasing the AAM. The role played by frictional torques in the 50-day oscillations in the AAM was first pointed out by Madden [1987] and confirmed by Weickmann *et al.* [1992]. Magaña [1993] documented 40- to 50-day oscillations in the AAM in the extratropics of both hemispheres, which might occur independently of the tropical oscillation. However, Anderson and Rosen [1983] have shown that the 40- to 50-day

Copyright 1998 by the American Geophysical Union.

Paper number 98JD01145.  
0148-0227/98/98JD-01145\$09.00

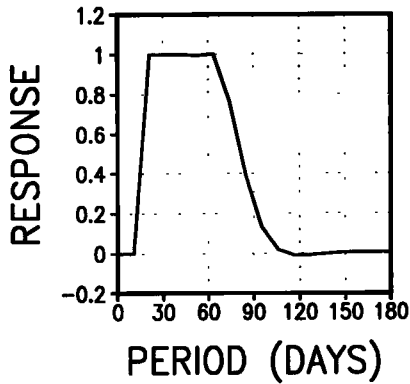


**Figure 1.** Lanczos filter response for the intraseasonal band-pass filter.

oscillations in the relative angular momentum propagate upward and out of the tropics to the midlatitudes.

Several authors have gathered observational evidence of interactions between the tropical and extratropical oscillations in the IS timescale [Weickmann *et al.*, 1985; Knutson and Weickmann, 1987; Murakami, 1987]. Weickmann *et al.* [1985] found statistically significant relationships between the IS variations in the tropical OLR and the 250-hPa planetary-scale circula-

tion features during the northern hemisphere (NH) winter. They found that the global circulation associated with the eastward propagating OLR anomalies includes an eccentric 250-hPa circumpolar vortex in the NH extratropics, expanded in the regions of equatorial cloudiness and subtropical anticyclones and contracted in the regions of suppressed equatorial cloudiness and subtropical cyclones. Knutson and Weickmann [1987] extended Weickmann *et al.*'s [1985] results and found that zonally elongated zonal wind perturbations (anomalous easterlies) over southern Australia and between 50°S and 70°S accompany the negative OLR anomalies over Indonesia and the western Pacific during the SH winter. Murakami [1987] showed that the amplitude of the extratropical response to variations in the convection is larger for periods when the OLR anomalies propagate eastward from the Indian Ocean to the central Pacific. In a recent paper, Zhang and Hendon [1997] analyzed the propagating and standing components of the IS oscillation in tropical convection but failed to identify any dominant standing oscillation.

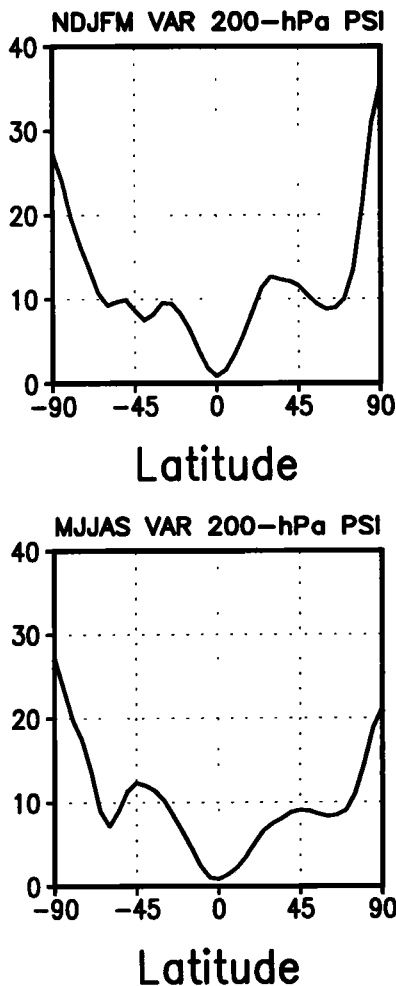


**Figure 2.** Seasonal variances for the zonally symmetric 200-hPa stream function. The variance unit is  $10^{12} \text{ m}^4 \text{ s}^{-2}$ .

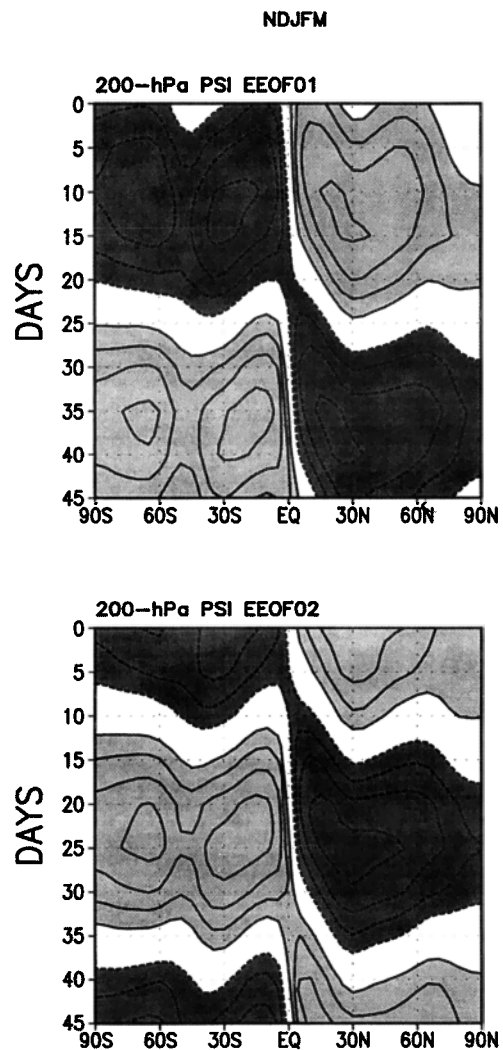


**Figure 3.** Northern hemisphere (NH) winter (November-March) first two extended empirical orthogonal function (EOF) modes for zonally symmetric filtered 200-hPa stream function. Contour interval is 0.2. Lighter (darker) shading indicates loadings greater (less) than 0.2 ( $-0.2$ ). Zero line is not shown.

## NDJFM SLP COR EEOF 01

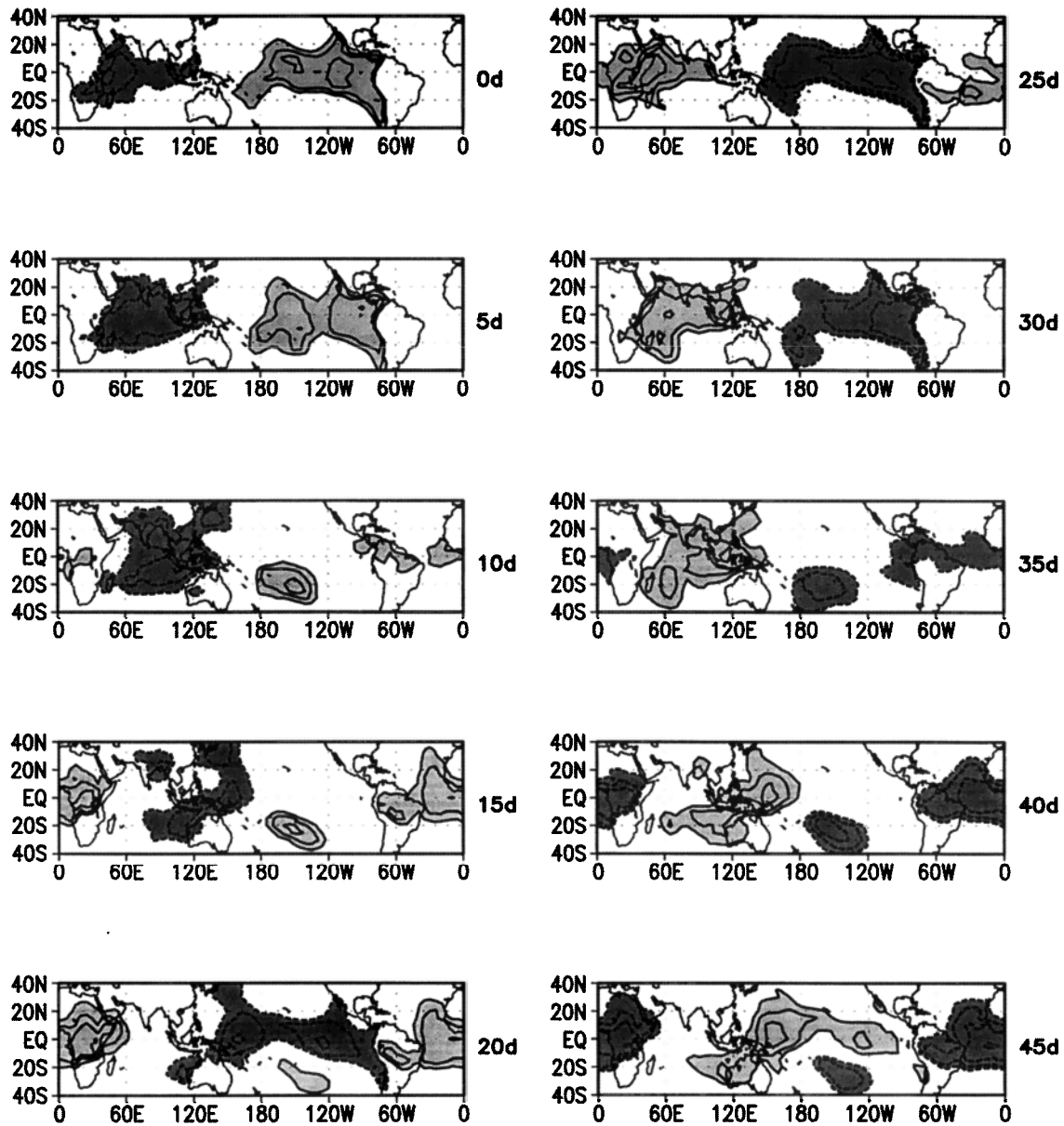


**Figure 4.** NH winter zonally asymmetric sea level pressure (SLP) patterns associated with the EEOF mode-1 shown in Figure 3. The values are correlations between the filtered anomaly time series at each grid point for winter and the amplitude time series for the EEOF mode 1. Contour interval is 0.1. Lighter (darker) shading indicates correlations greater (less) than 0.3 ( $-0.3$ ). Lines from  $-0.2$  to  $0.2$  are not shown.

*Knutson and Weickmann* [1987] suggested that the extratropical basic state circulation plays an important role in the tropical-extratropical interactions. The present paper focuses on this aspect by determining the evolving IS features of the zonally symmetric (ZS) upper tropospheric stream function and the associated IS patterns of the zonally asymmetric (ZA) part of selected variables. The variables used in this study are the same as those in previous works [e.g., *Weickmann et al.*, 1985] that exhibit strong zonal symmetry in their IS patterns. This justifies the decomposition of the variables into their ZS and ZA components.

## 2. Data and Methodology

The data set consists of nonoverlapping 5-day (pentad) means for atmospheric variables extracted from the reanalyzed fields provided by the Climate Data Assimilation System (CDAS) Reanalysis Project [*Kalnay et al.*, 1996]. Pentad means of the zonal wind at 850 and at 200 hPa, the 200-hPa stream function, and the SLP for the January 1979 to June 1996 period are used in this study. These data have a resolution of  $2.5^\circ$  in latitude and longitude. Owing to computational limitations, the data resolution is reduced to  $5^\circ$  in latitude and longitude by

## NDJFM 850-hPa U COR EEOF 01

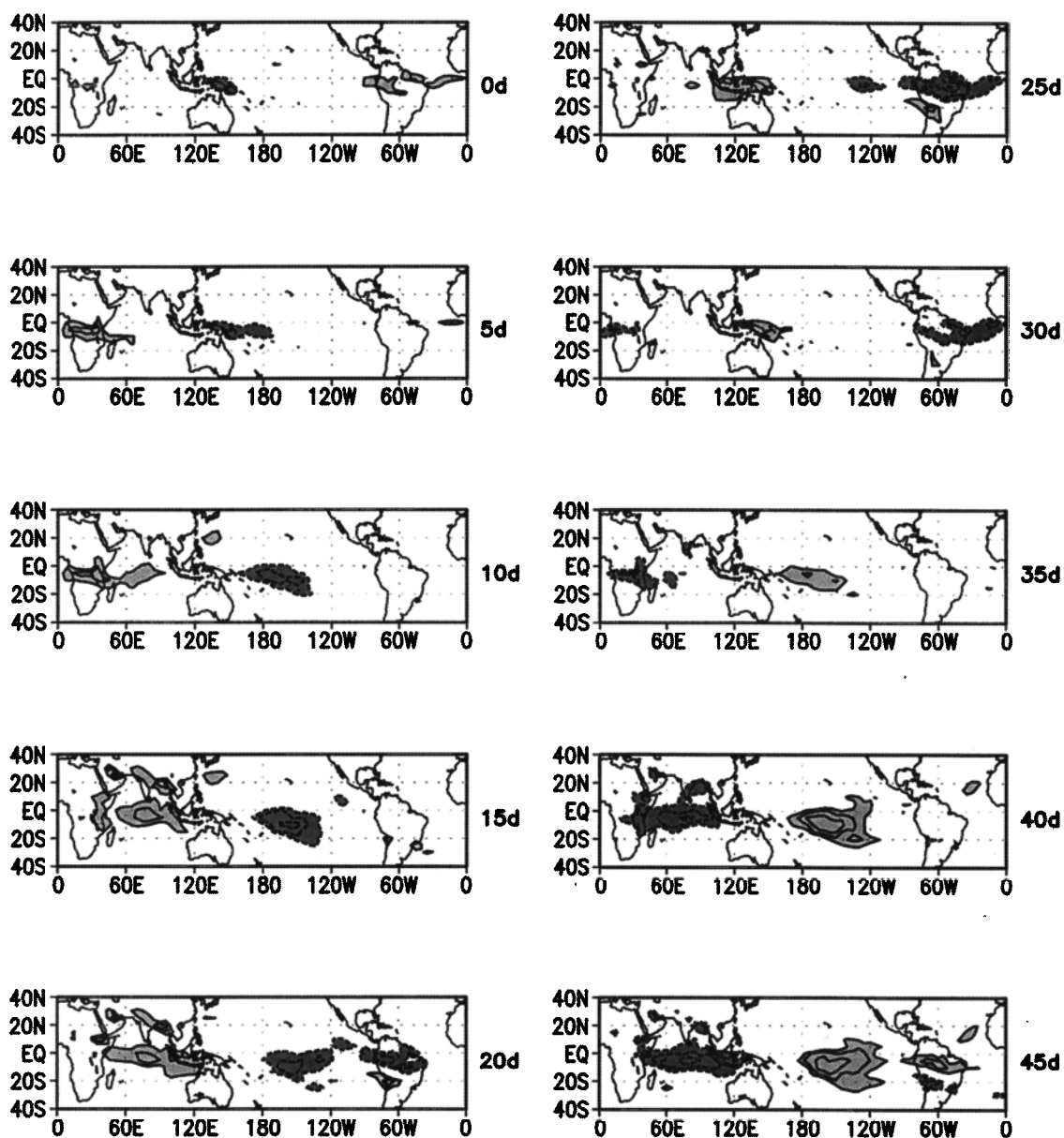


Figure 5. Same as Figure 4, except for the zonally asymmetric 850-hPa zonal wind.

sampling the variables every other grid point. Anomalies for each variable are calculated with respect to the 1979–1995 base period pentad means. These anomaly time series are then decomposed in the ZS and ZA parts.

The data are temporally filtered using a Lanczos band-pass filter [Duchon, 1979], with 97 weights and cutoff frequencies of 0.2 and  $0.0575 \text{ pentad}^{-1}$ . This filter has been previously used by Kousky and Kayano [1994] in a study of IS variability for the South American region. The frequency response function of this filter (Figure 1) shows that the amplitudes of oscillations with periods between 20 and 70 days are not altered.

To perform the extended empirical orthogonal function (EEOF) analysis [Weare and Nasstrom, 1982], the 200-hPa ZS stream function (filtered anomaly) profiles are extended to include a total of 10 different time lags with a lag interval of 1

pentad. This analysis reveals the evolving aspects of the 200-hPa ZS stream function. The associated ZA patterns for each mode for selected variables (850- and 200-hPa zonal winds and sea level pressure (SLP)) are obtained by linearly correlating the respective principal component time series of the EEOF analysis for the 200-hPa ZS stream function with ZA filtered anomaly time series for each selected variable at every grid point. The spatial patterns of the ZA component for each variable are also extended to include 10 different time lags. Correlation coefficients are calculated separately for each ZA variable in the area between  $80^{\circ}\text{N}$  and  $80^{\circ}\text{S}$  around the globe. Ten correlation patterns, one for each lag interval, are obtained for each EEOF mode for each variable.

To assess the statistical significance of having a correlation coefficient different from zero, the number of degrees of free-

## NDJFM 200-hPa U COR EEOF 01

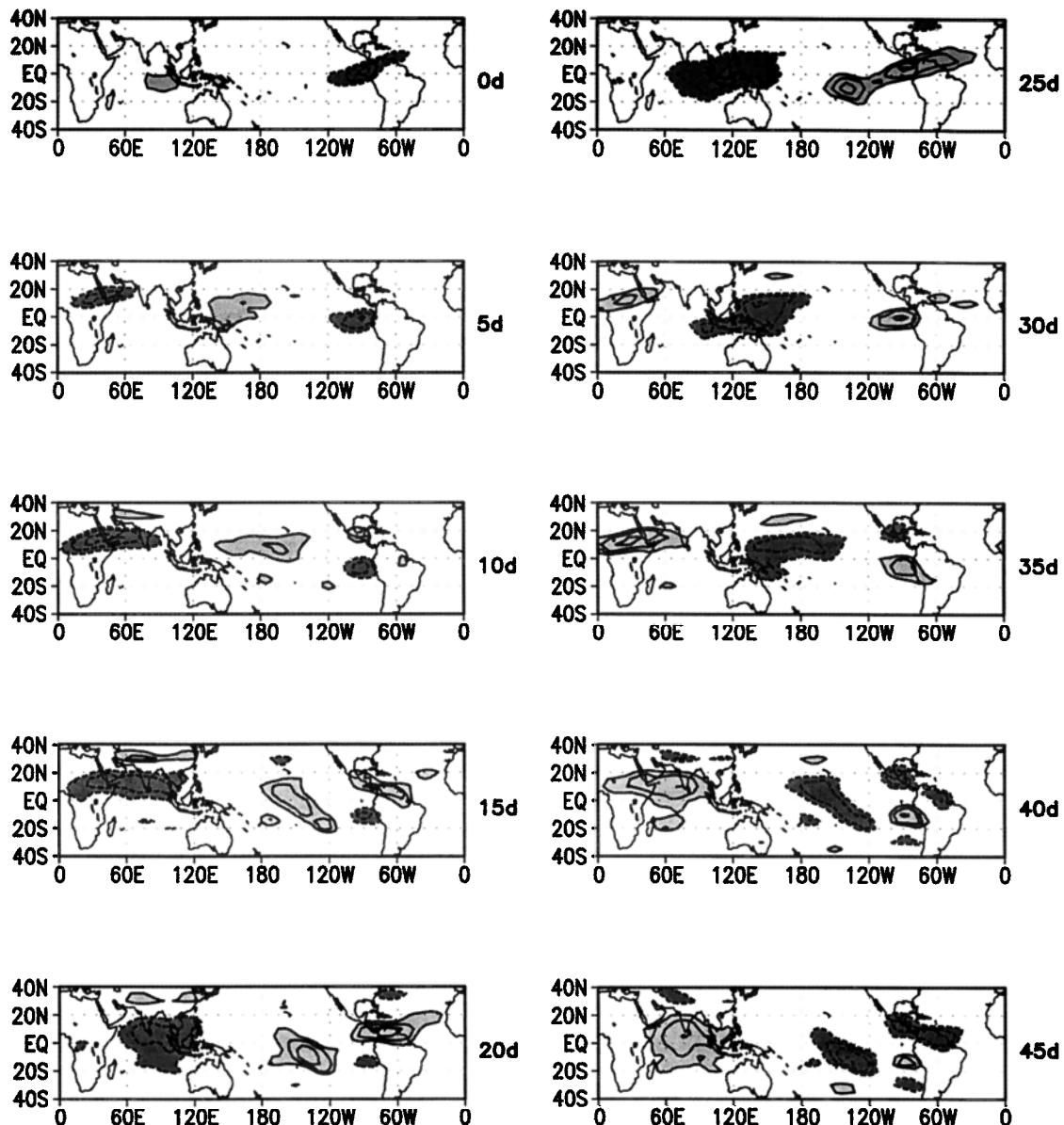


Figure 6. Same as Figure 4, except for the zonally asymmetric 200-hPa zonal wind.

dom has been estimated using the method of *Zhang and Hendon* [1997]. The result is 40 degrees of freedom, which is the total number of pentads in a time series: 480 (16 years  $\times$  30 pentads for a season) divided by 12 (the number of pentads for a 60-day period). Using a two-tailed student's *t*-test, it is found that correlations  $>0.26$  are significantly different from zero correlation at the 90% level of significance. So only correlations  $>0.3$  are considered in our analysis.

The EEOF calculations are based on the correlation matrix and are done separately for the NH summer (May–September (MJJAS)) and winter (November–March (NDJFM)). The same number of summers and winters is analyzed by choosing the 16 MJJAS periods included in the years from 1980 to 1995 for summer and the 16 NDJFM periods from 1979 to 1995 for winter. The correlation matrix was chosen to perform the

EEOF calculations based on the analysis of seasonal variances of the filtered 200-hPa ZS stream function (Figure 2). The largest variances are found in high latitudes, with larger values in the winter hemisphere. Eigenstructure calculations based on the covariance matrix would emphasize the patterns in high latitudes, where the IS variance is large. In contrast, eigenstructure calculations based on the correlation matrix provide the joint variance structure of the standardized variables. For this reason, the method of calculating the EEOF based on the correlation matrix was adopted. The reader's attention is called to the fact that the variances of the filtered 200-hPa ZS stream function are considerably smaller than the total variance calculated with unfiltered data.

An important point to be considered in using EOF or EEOF analyses is the physically meaningful identity of a given mode.

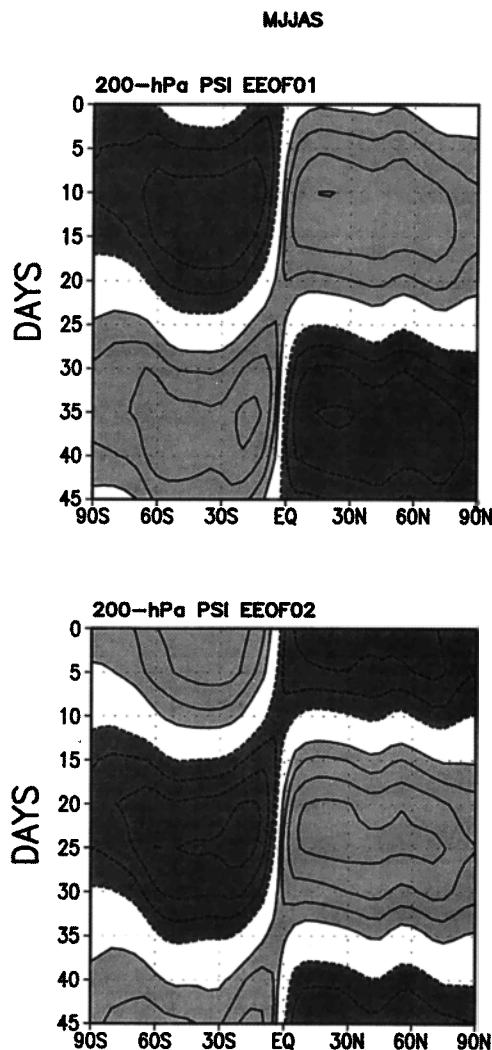


**Figure 7.** NH summer (May–September) first two EEOF modes for zonally symmetric filtered 200-hPa stream function. Display is the same as in Figure 3.

According to the method proposed by *North et al.* [1982], a given mode  $n$  can be elected as a physically meaningful identity if the associated eigenvalue  $\lambda_n$  is well separated from the neighboring ones, that is,  $\delta\lambda_{n-1} < \Delta\lambda_{n-1}$  and  $\delta\lambda_n < \Delta\lambda_n$ , where  $\delta\lambda_n$  ( $\sim \lambda_n (2/N)^{1/2}$ ) is the sampling error of  $\lambda_n$ ,  $N$  is the degrees of freedom, and  $\Delta\lambda_n (= \lambda_n - \lambda_{n+1})$  is the spacing between eigenvalues. If two adjacent eigenvalues are clustered but well separated from their neighboring eigenvalues, then their modes may be combined to yield a physically meaningful pattern.

### 3. Results

Using *North et al.* [1982] separation criteria for each analysis (summer and winter), it is found that the first two EEOF modes for the 200-hPa ZS stream function are not separated from each other but well separated from the higher modes. Thus these two modes describe physically meaningful evolving patterns. The EEOF technique emphasizes the cyclical behavior of the evolution of anomaly patterns. Therefore, for each evolving pattern, the analysis results in two modes that describe a similar evolution but with the patterns, for a fixed time,

90° out of phase. It will be shown that the first two modes of each analysis (summer and winter) indeed form a pair that describes a similar evolution.

The EEOF modes for the 200-hPa ZS stream function consist of 10 latitudinal profiles (one for each lag interval), which have been displayed in lag interval versus latitude plots. The associated ZA patterns for the SLP and the 850- and 200-hPa zonal winds have been shown only equatorward of 40°, since outside this latitude band no statistically significant correlations have been found. For these patterns, only correlations  $>0.3$  are contoured in the corresponding figures.

#### 3.1. NH Winter EEOF for the 200-hPa ZS Stream Function

The first two NH winter EEOF modes for the 200-hPa ZS stream function together account for 52% of the total IS variability. It is evident that these two modes (Figure 3) describe a similar evolution of the latitudinal 200-hPa ZS stream function profiles; therefore, for brevity, only the first mode is discussed. The latitudinal 200-hPa ZS stream function profiles for the first mode on days 5–10 are approximately reversed with respect to those on days 30–35 (Figure 3), thus implying a period of approximately 50 days for this mode. These profiles show a temporal evolution with the largest loadings, near the equator in both hemispheres, propagating poleward and reaching subtropical latitudes. It is also worth noting some indications of an equatorward propagation of the loadings poleward of 30°N.

The profiles in the tropical latitudes, where the loadings are the largest, are nearly antisymmetric about the equator. High (low) stream function corresponds to high (low) geopotential height in the NH and low (high) geopotential height in the SH. Thus the meridional gradient of geopotential height as evidenced by positive (negative) loadings in the NH and negative (positive) loadings in the SH implies equatorial anomalous easterlies (westerlies).

#### 3.2. NH Winter ZA Patterns

The NH winter ZA patterns for the SLP and for the 850- and 200-hPa zonal winds associated with the first NH winter ZS EEOF mode are shown in Figures 4, 5, and 6, respectively. The patterns observed on days 15 and 40 are approximately reversed, implying a 50-day period oscillation. The general feature of these patterns is a large-scale zonal wavenumber one structure in the tropics propagating continuously eastward around the globe. The dominant SLP patterns (Figure 4) are, in general, nearly symmetric about the equator. Exceptions are noted, in the central Pacific, where the patterns extend south-eastward along the South Pacific convergence zone (SPCZ), and in the equatorial eastern Pacific, where the largest correlation values extend along the western South American coast.

Statistically significant correlations for the 850-hPa ZA zonal wind (Figure 5) are found for certain time lags, being confined in relatively small areas. These areas are approximately symmetric about 5°S, that is, the average latitude of the equatorial trough during the NH winter. The low-level east-west oriented dipole is better defined at those times when one center is located in the Indian Ocean and the other in the central and eastern Pacific. The 200-hPa ZA zonal wind patterns (Figure 6) feature the largest correlations over the tropical Indian Ocean, Indonesia, equatorial western Pacific, and northern South America and Central America and their adjoining oceanic areas. Except over Indonesia, these patterns are approximately symmetric about 5°N–10°N. For some time

MJJAS SLP COR EEOF 01

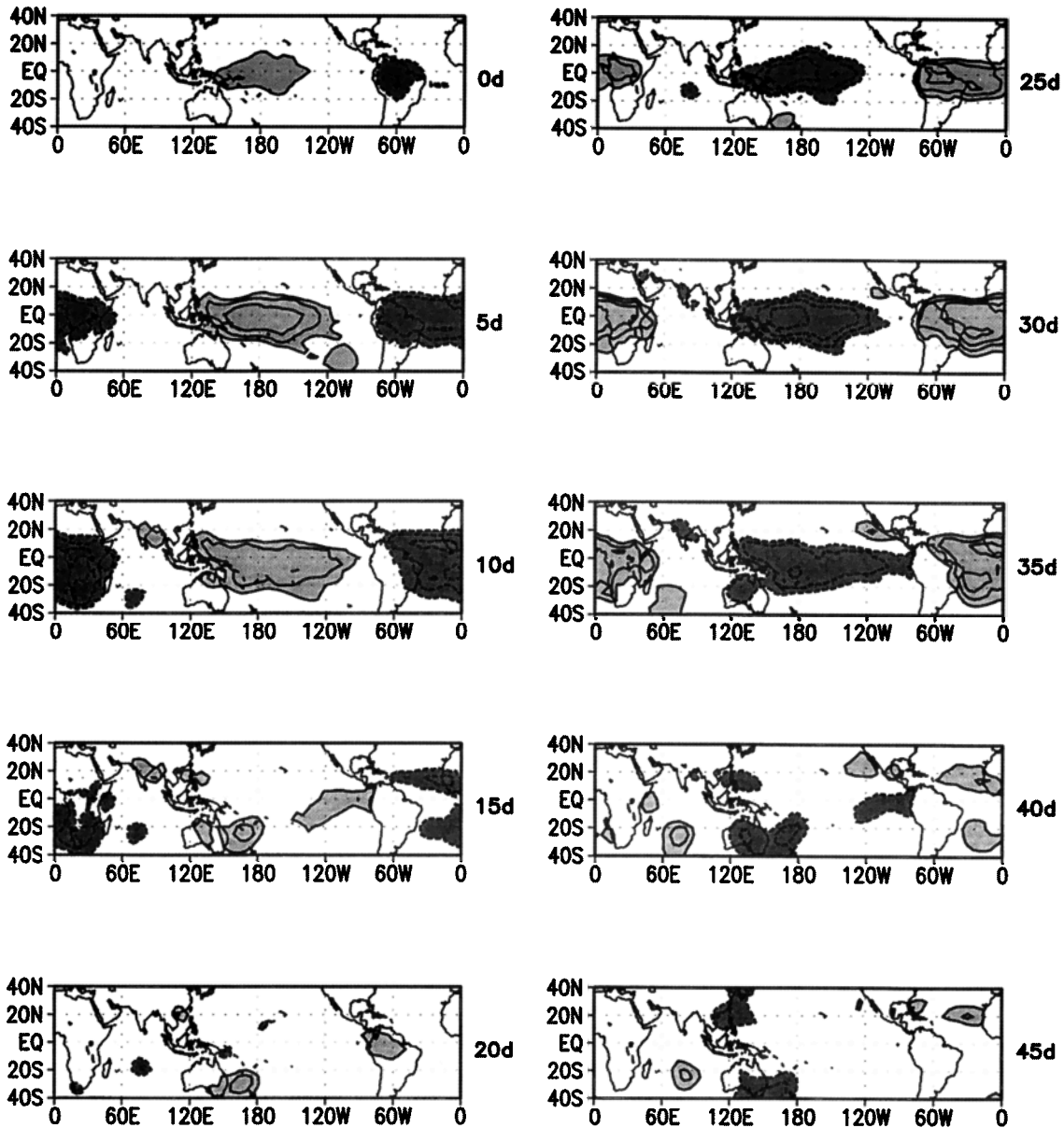


**Figure 8.** NH summer zonally asymmetric SLP patterns associated with the EEOF mode-1 shown in Figure 7. The values are correlations between the filtered anomaly time series at each grid point for summer and the amplitude time series for the EEOF mode 1. Display is the same as in Figure 4.

lags the 200-hPa ZA zonal wind patterns show an extension along the SPCZ.

**3.3. NH Summer EEOF for the ZS 200-hPa Stream Function**

The first two NH summer EEOF modes for the 200-hPa ZS stream function together explain 51% of the total IS variability (Figure 7). Similar to the NH winter mode, it is evident these two modes describe a similar evolution of the latitudinal 200-hPa ZS stream function profiles; therefore, for brevity, only the first mode is discussed. The first two NH summer modes describe a 50-day oscillation period. The 200-hPa ZS stream function profiles have the largest loadings approximately anti-

symmetric about the equator and for the latitudes within the 30°S–30°N band. As for the NH winter mode, the largest loadings near the equator in both hemispheres show a poleward propagation.

**3.4. NH Summer ZA Patterns**

The NH summer ZA patterns for the SLP and for the 850- and 200-hPa zonal winds associated with the first NH summer 200-hPa ZS stream function EEOF mode are shown in Figures 8, 9, and 10, respectively. The general characteristics of these patterns are similar to those for the corresponding winter ZA patterns. Namely, the largest correlations are confined to the tropics, with a large-scale zonal wavenumber one structure

## MJJAS 850-hPa U COR EEOF 01

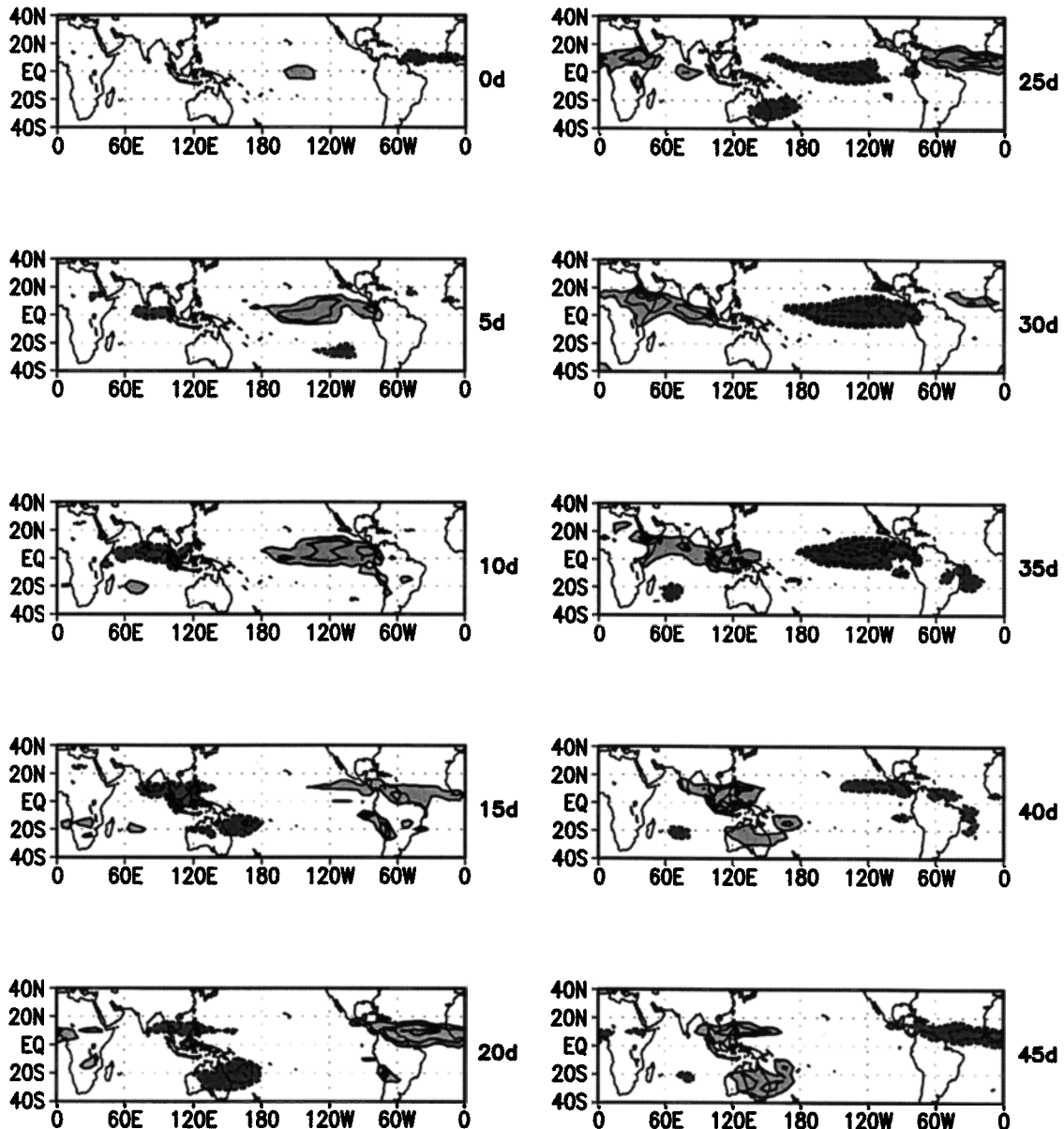


Figure 9. Same as Figure 8, except for the zonally asymmetric 850-hPa zonal wind.

propagating continuously eastward around the globe with a 50-day period. For some time lags the SLP patterns (Figure 8) show a strong symmetry about the equator and a well-defined east-west dipole, with one center located in the equatorial western Pacific and the other within an area extending eastward from northern South America to equatorial Africa.

The 850-hPa ZA zonal wind patterns (Figure 9) depict the largest correlations symmetric about  $10^{\circ}\text{N}$  in an area extending eastward from the Atlantic to the western Pacific and about the equator in the central and eastern Pacific. These areas are approximately coincident with the seasonal position of the Intertropical Convergence Zone (ITCZ). The east-west dipole in the 850-hPa ZA zonal wind correlation patterns is relatively better defined at certain times for which one center is found

over the equatorial Indian Ocean and the other in the equatorial eastern Pacific.

The 200-hPa ZA zonal wind patterns (Figure 10) feature the largest correlations over the Indian Ocean–Indonesia region, the equatorial eastern Pacific, and the equatorial Atlantic. Thus, except for small areas over Africa and Australia, the largest correlations are found mainly over oceanic areas. It is also interesting to note that throughout the evolution the largest loadings are mostly confined to over Indonesia.

#### 4. Concluding Remarks

The evolving intraseasonal (IS) modes of the zonally symmetric (ZS) part of the 200-hPa stream function have been

## MJJAS 200-hPa U COR EEOF 01

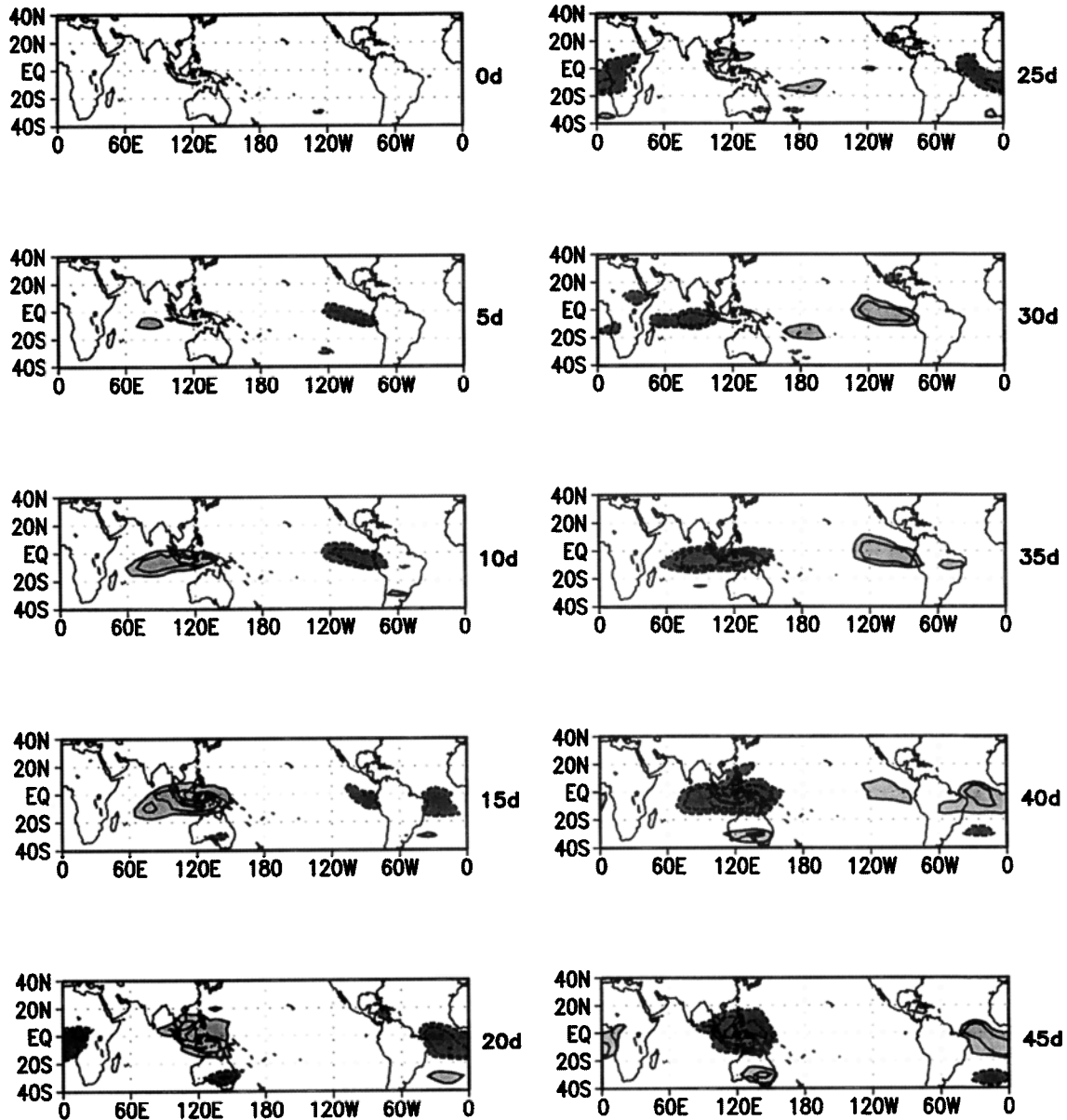


Figure 10. Same as Figure 8, except for the zonally asymmetric 200-hPa zonal wind.

determined by performing EEOF analyses separately for the NH summer (May–September) and the NH winter (November–March) data. For both analyses the first two EEOF modes describe a similar evolution of the latitudinal 200-hPa ZS stream function profiles. Thus only the first mode of each analysis is discussed, and the associated patterns for the zonally asymmetric (ZA) part of the 850- and 200-hPa zonal winds and SLP are determined.

For both seasons the first EEOF profiles for the 200-hPa ZS stream function describe a 50-day oscillation period. The prominent feature of these profiles is the propagation of the largest loadings near the equator in both hemispheres toward higher latitudes. This propagation is more pronounced during the NH winter and throughout the year in the SH, and it is noticeable in the latitudes within the 30°S–30°N band. It is also

worth noting that the profiles within this band are nearly antisymmetric about the equator.

Since high (low) stream function corresponds to high (low) geopotential height in the NH and low (high) geopotential height in the SH, the variations in the north–south distribution of the largest loadings due to their poleward propagation indeed represent variations in the meridional gradient of geopotential height and consequently in the zonal winds.

Variations in the zonal winds, in particular in the tropics, have been related to the 50-day oscillations in the atmospheric angular momentum (AAM) [e.g., *Benedict and Haney, 1988; Gutzler and Madden, 1993*]. Thus the propagation of the largest loadings of the upper level ZS stream function in both hemispheres from near equatorial latitudes toward higher latitudes might be an indication of the meridional propagation of the 40-

to 50-day oscillation in the AAM previously documented [e.g., Anderson and Rosen, 1983; Magaña, 1993].

On the other hand, the ZA patterns for the SLP and the 850- and 200-hPa zonal winds for both seasons feature the largest correlations in the tropics and a zonal wavenumber one structure propagating continuously eastward around the globe with a 50-day period. It is worth noting that the ZA patterns show strong seasonal dependence. The 850-hPa ZA zonal wind patterns feature the largest correlations approximately along the climatological position of the ITCZ. This suggests that the MJO-related variations in the ITCZ convection are closely linked to variations in the low-level ZA zonal winds. The upper level ZA zonal wind patterns exhibit the largest correlations near the equator but mainly in the winter hemisphere.

To gain more confidence in our results, combined EEOF analyses of the (filtered) ZA part of the 850- and 200-hPa zonal winds and SLP have also been performed (not shown). For both seasons the first mode patterns for these analyses are quite similar to those discussed in sections 3.2 and 3.4. Therefore the eastward traveling aspects of the MJO (as revealed in the 850- and 200-hPa zonal winds and the SLP), although strongly related to the ZA component of the circulation, are also closely related to the ZS component of the circulation.

**Acknowledgments.** The authors thank two anonymous reviewers for their helpful comments and suggestions. The first author was partially supported by the Conselho Nacional de Desenvolvimento Científico e Tecnológico under grant 300033/94-0.

## References

- Anderson, J. R., and R. D. Rosen, The latitude-height structure of 40–50 day variations in atmospheric angular momentum, *J. Atmos. Sci.*, **40**, 1584–1591, 1983.
- Anderson, J. R., and D. E. Stevens, The presence of linear wavelike modes in a zonally symmetric model of the tropical atmosphere, *J. Atmos. Sci.*, **44**, 2115–2127, 1987.
- Benedict, W. L., and R. L. Haney, Contribution of tropical winds to subseasonal fluctuations in atmospheric angular momentum and length of day, *J. Geophys. Res.*, **93**, 15,973–15,978, 1988.
- Duchon, C. E., Lanczos filtering in one and two dimensions, *J. Appl. Meteorol.*, **18**, 1016–1022, 1979.
- Ghil, M., and K. Mo, Intraseasonal oscillations in the global atmosphere, I, Northern hemisphere and tropics, *J. Atmos. Sci.*, **48**, 752–779, 1991a.
- Ghil, M., and K. Mo, Intraseasonal oscillations in the global atmosphere, II, Southern hemisphere, *J. Atmos. Sci.*, **48**, 780–790, 1991b.
- Gutzler, D. S., and R. A. Madden, Seasonal variations of the 40–50 day oscillation in atmospheric angular momentum, *J. Atmos. Sci.*, **50**, 850–860, 1993.
- Higgins, H. W., and K. C. Mo, Persistent North Pacific circulation anomalies and the tropical intraseasonal oscillation, *J. Clim.*, **10**, 223–244, 1997.
- Kalnay, E., et al., The NCEP/NCAR 40-year reanalysis project, *Bull. Am. Meteorol. Soc.*, **77**, 437–471, 1996.
- Kang, I.-S., and K.-M. Lau, Evolution of tropical circulation anomalies associated with 30–60 day oscillation of globally averaged angular momentum during northern summer, *J. Meteorol. Soc. Jpn.*, **68**, 237–249, 1990.
- Kiladis, G. N., and K. M. Weickmann, Circulation anomalies associated with tropical convection during northern winter, *Mon. Weather Rev.*, **120**, 1900–1923, 1992.
- Knutson, T. R., and K. M. Weickmann, 30–60 day atmospheric oscillations: Composite life cycles of convection and circulation anomalies, *Mon. Weather Rev.*, **115**, 1407–1436, 1987.
- Knutson, T. R., K. M. Weickmann, and J. E. Kutzbach, Global-scale intraseasonal oscillation of outgoing longwave radiation and 250-mb zonal wind during northern hemisphere summer, *Mon. Weather Rev.*, **114**, 605–623, 1986.
- Kousky, V. E., and M. T. Kayano, Principal modes of outgoing longwave radiation and 250-mb circulation for the South American sector, *J. Clim.*, **7**, 1131–1143, 1994.
- Langley, R. B., R. W. King, I. I. Shapiro, R. D. Rosen, and D. A. Salstein, Atmospheric angular momentum and the length of day: A common fluctuation with a period near 50 days, *Nature*, **294**, 730–732, 1981.
- Lau, K.-M., and P. H. Chan, Aspects of the 40–50 day oscillation during the northern winter as inferred from outgoing longwave radiation, *Mon. Weather Rev.*, **113**, 1889–1909, 1985.
- Lorenc, A. C., The evolution of planetary-scale 200-mb divergent flow during the FGGE year, *Q. J. R. Meteorol. Soc.*, **110**, 427–441, 1984.
- Madden, R. A., Seasonal variations of the 40–50 day oscillation in the tropics, *J. Atmos. Sci.*, **43**, 3138–3158, 1986.
- Madden, R. A., Relationship between changes in the length of day and the 40- to 50-day oscillation in the tropics, *J. Geophys. Res.*, **92**, 8391–8399, 1987.
- Madden, R. A., and P. R. Julian, Detection of a 40–50 day oscillation in the zonal wind in the tropical Pacific, *J. Atmos. Sci.*, **28**, 702–708, 1971.
- Madden, R. A., and P. R. Julian, Description of global-scale circulation cells in the tropics with a 40–50 day period, *J. Atmos. Sci.*, **29**, 1109–1123, 1972.
- Madden, R. A., and P. R. Julian, Observations of the 40–50 day tropical oscillation: A review, *Mon. Weather Rev.*, **122**, 814–837, 1994.
- Magaña, V., The 40- and 50-day oscillations in atmospheric angular momentum at various latitudes, *J. Geophys. Res.*, **98**, 10,441–10,450, 1993.
- Mo, K. C., and V. E. Kousky, Further analysis of the relationship between circulation anomaly patterns and tropical convection, *J. Geophys. Res.*, **98**, 5103–5113, 1993.
- Murakami, T., Intraseasonal atmospheric teleconnection patterns during the northern hemisphere summer, *Mon. Weather Rev.*, **115**, 2133–2154, 1987.
- North, G. R., T. L. Bell, R. F. Cahalan, and F. J. Moeng, Sampling errors in the estimation of empirical orthogonal functions, *Mon. Weather Rev.*, **110**, 699–706, 1982.
- Rosen, R. D., and D. A. Salstein, Variations in atmospheric angular momentum on global and regional scales and the length of day, *J. Geophys. Res.*, **88**, 5451–5470, 1983.
- Weare, B. C., and J. S. Nasstrom, Example of extended orthogonal function analysis, *Mon. Weather Rev.*, **110**, 481–485, 1982.
- Weickmann, K. M., Intraseasonal circulation and outgoing longwave radiation modes during the northern hemisphere winter, *Mon. Weather Rev.*, **111**, 1838–1858, 1983.
- Weickmann, K. M., G. R. Lussky, and J. E. Kutzbach, A global-scale analysis of intraseasonal fluctuations of outgoing longwave radiation and 250-mb stream function during northern winter, *Mon. Weather Rev.*, **113**, 941–961, 1985.
- Weickmann, K. M., S. J. S. Khalsa, and J. E. Eischeid, The atmospheric angular momentum cycle during the tropical Madden-Julian oscillation, *Mon. Weather Rev.*, **120**, 2252–2263, 1992.
- Zhang, C., and H. H. Hendon, Propagating and standing components of the intraseasonal oscillation in tropical convection, *J. Atmos. Sci.*, **54**, 741–752, 1997.

M. T. Kayano, Instituto Nacional de Pesquisas Espaciais, C.P. 515, 12201-970 São José dos Campos, SP, Brazil. (e-mail: mary@met.inpe.br)

V. E. Kousky, Climate Prediction Center, National Centers for Environmental Prediction, 5200 Auth Road, Room 605, Camp Springs, MD 20746. (e-mail: wd52vk@hp31.wvb.noaa.gov)

(Received August 18, 1997; revised March 16, 1998; accepted April 1, 1998.)